



Published in final edited form as:

*J Mol Neurosci.* 2014 December ; 54(4): 630–638. doi:10.1007/s12031-014-0347-y.

## Molecular neuroimaging of post-injury plasticity

Yan Jouroukhin<sup>1,2</sup>, Bareng A. S. Nonyane<sup>3</sup>, Assaf A. Gilad<sup>1,2,4</sup>, and Galit Pelled<sup>1,2,\*</sup>

<sup>1</sup>F.M. Kirby Research Center for Functional Brain Imaging, Kennedy Krieger Institute, Baltimore, Maryland, 21205, USA

<sup>2</sup>Russell H. Morgan Department of Radiology, Johns Hopkins University School of Medicine, Baltimore, Maryland, 21205, USA

<sup>3</sup>Department of International Health, Johns Hopkins Bloomberg School of Public Health, Baltimore, Maryland, 21205, USA

<sup>4</sup>Cellular Imaging Section and Vascular Biology Program, Institute for Cell Engineering, The Johns Hopkins University School of Medicine, Baltimore, Maryland, 21205, USA

### Abstract

Nerve injury induces long-term changes in neuronal activity in the primary somatosensory cortex (S1), which has often been implicated as the origin of sensory dysfunction. However, the cellular mechanisms underlying this phenomenon remain unclear. *C-fos* is an immediate early gene, which has been shown to play an instrumental role in plasticity. By developing a new platform to image real-time changes in gene expression *in vivo*, we investigated whether injury modulates the levels of *c-fos* in layer V of S1, since previous studies have suggested that these neurons are particularly susceptible to injury.

The yellow fluorescent protein, ZsYellow1, under the regulation of the *c-fos* promoter, was expressed throughout the rat brain. A fiber-based confocal microscope that enabled deep brain imaging was utilized and local field potential were collected simultaneously. In the weeks following limb denervation in adult rats (n=10), sensory stimulation of the intact limb induced significant increases in *c-fos* gene expression in cells located in S1, both contralateral (affected, 27.6±3 cells) and ipsilateral (8.6±3 cells) to the injury, compared to controls (n=10, 13.4±3 and 1.0±1, respectively, p-value <0.05). Thus, we demonstrated that injury activates cellular mechanisms that are involved in reshaping neuronal connections and this may translate to neurorehabilitative potential.

### Keywords

Immediate early genes; plasticity; injury; somatosensory cortex; optical imaging; gene expression

---

\*Corresponding author: Galit Pelled, The F.M. Kirby Center for Functional Brain Imaging, Kennedy Krieger Institute, Johns Hopkins School of Medicine, 707 N. Broadway, Baltimore, MD 21205. Tel: 443-923-2751. Pelled@kennedykrieger.org.

## Introduction

Sensory dysfunctions and chronic pain are a common complication in patients who have suffered peripheral nerve injury. Despite refined surgical techniques, the clinical outcome in adults is generally poor, with persisting sensory and pain problems (Lundborg, 2003). Previously, we demonstrated that neurons located in layer V of the affected primary somatosensory cortex (S1) (contralateral to the injured limb) are specifically vulnerable to injury (Pelled et al., 2009; Han et al., 2013). Moreover, it appears that the neuronal population in layer V that shows the greatest changes in firing rate post-injury are the inhibitory interneurons (Pelled et al., 2009; Li et al., 2011). These long-term changes in the balance between excitation and inhibition could potentially have an adverse effect on neurorehabilitation. Yet, the cellular mechanisms leading to this phenomenon remain unknown. We hypothesize that injury modulates levels of gene expression that may be involved in reshaping neuronal connections as well.

Long-term plasticity changes require a variety of molecular and cellular mechanisms, among them the activation of transcription factors encoded by immediate early genes (IEG), which are dynamically regulated by neuronal activity. One of the IEG is the *fos* gene family (Milde-Langosch, 2005), which is expressed rapidly and transiently in neurons in response to stimuli. *C-fos* has been shown to play an instrumental role in plasticity, for example, mice lacking the *c-fos* gene demonstrate impaired hippocampal-dependent learning and memory (Fleischmann et al., 2003), and impaired acquisition and consolidation of aversive taste learning (Yasoshima et al., 2000). Successful efforts have yielded a generation of transgenic mice and rats expressing reporters fused to the *c-fos* gene, such as  $\beta$ -gal (Kasof et al., 1995; Wilson et al., 2002), green fluorescent protein (GFP) (Barth et al., 2004; Cifani et al., 2012), and monomeric red fluorescent protein-1 (Fujihara et al., 2009). Recently, a new approach that enables the inducible expression of *c-fos* has been developed and used to study memory retrieval in mice (Reijmers et al., 2007; Liu et al., 2012). Nevertheless, thus far, visualization of *c-fos* expression has been limited to post-mortem assessment and superficial changes in cortical structure (Wada et al., 2010) using traditional microscopy techniques.

We have capitalized on recent progress in microscopy and molecular imaging technologies and developed a platform to image real-time changes in *c-fos* activity in deep brain areas. We constructed a lentivirus encoding to the yellow fluorescent protein, ZsYellow1, under the regulation of the *c-fos* promoter, and expressed it throughout the rat brain. A fiber-based confocal microscope was used, which enabled *in vivo* imaging of deep brain structures (Pelled et al., 2006). Our results show that post-injury plasticity involves increases in transcription levels of *c-fos* in layer V of S1, both contralateral and ipsilateral to the injured limb.

## Material and Methods

All animal procedures were conducted in accordance with the NIH Guide for the Care and Use of Laboratory Animals and were approved by the Johns Hopkins University Animal Care and Use Committee.

## Cloning and lentivirus production

Lentiviral vector carrying the reporter gene (ZsYellow1, Clontech), under the regulation of the *c-fos* promoter, were constructed using ViraPower Promoterless Lentiviral Gateway kit (K591-10, Invitrogen). *C-fos* promoter containing the first intron in addition to promoter elements (position -379 to +119 with respect to the *c-fos* gene (Susini et al., 2000)) was produced by PCR amplification (primers: 5'-TCGCACCCTCAGAGTTGG-3' and 5'-TTGGGGAAAGCCCGCAA-3') from rat genomic DNA (catalog No. 636404, Clontech) (Susini et al., 2000), and cloned into a pENTR5' vector. Both pENTR5'-*c-fos* and pENTR1A-ZsYellow1 (fused to the V5 epitope) underwent LR recombination into the destination vector pLenti-6-V5/DEST. The new recombinant destination vectors, pLenti-6-*c-fos*-ZsYellow1-V5, were packaged into a VSV-G pseudotype lentivirus.

The lentivirus particles were produced by transient transfection of 293FT cells with the constructed vector, psPAX.2 (#12260, Addgene) and pMD2.G (#12259, Addgene) plasmids, at a ratio of 6:2:1 using Lipofectamine 2000 (#11668-019, Invitrogen). High titer lentivirus (>10<sup>9</sup> TU/ml) was then used for *in vivo* delivery.

## Cell culture

SH-SY5Y human neuroblastoma cells were cultured in a 1:1 mixture of Dulbecco's modified Eagle's medium and an F12 base medium (10-092-CV, Corning Cellgro) with 10% fetal bovine serum (FBS, F4135, Sigma-Aldrich), 100 IU/ml penicillin, and 50 µg/ml streptomycin (Sigma-Aldrich, P0781). Transfections were performed using Lipofectamine 2000 (#11668019, Life Technologies) in 24-well plates. Prior to the experiments, cells were kept in serum-free medium for 36 hours. Cells transfected with pLenti-6-*c-fos*-ZsYellow1-V5 were imaged using an inverted fluorescent microscope (IX70, Olympus) and three sequential images were captured every 15 minutes. From each well, four fluorescent and bright-field fields of view were captured using a ×10 objective lens. Following three baseline images, medium containing 12-O-tetradecanoylphorbol-13-acetate (TPA final concentration 16 nM; #79346, Sigma), diluted in DMSO, or the same volume of DMSO, was added to wells in addition to FBS final concentrations of 10%. Subsequent images were captured at 15 min, 30 min, 45 min, 1h, 2h, and 4h. Nine to twelve cells from three independent experiments were chosen for fluorescence quantification throughout all time points using ImageJ software (NIH). The difference in mean normalization-to-background signal intensity between treated and non-treated cells was tested using the Wilcoxon signed ranks test.

## Animal model

Twenty two-day-old Sprague-Dawley rats were stereotaxically injected with 5 µl of lentivirus in the right lateral ventricle according to (Li et al., 2011). Rats were fixed into the stereotaxic apparatus under cryoanesthesia. Using a Benchmark digital stereotaxic control panel, injections were made precisely to the right lateral ventricle with these coordinates: 0.8 mm anterior-posterior (AM), 2 mm medial-lateral (ML); and 1.8 mm dorsal-ventral (DV), relative to bregma. The concentrated lentivirus was delivered using a 10-µl syringe and a 31-gauge metal needle. The injection flow rate was controlled with a Quintessential Stereotaxic Injector (Stoelting Co). Five-week-old rats expressing the lentiviral vector underwent

unilateral forepaw denervation by excision of the left forepaw radial, median, and ulnar nerves, as reported previously (n=10) (Pelled et al., 2007). Denervation was performed under 2% isoflurane anesthesia. During the week following the surgery, 1.5 ml/100 g of the opioid receptor agonist, tramadol hydrochloride, was administered orally twice a day. Twelve virus injected rats that did not undergo denervation served as the control group.

### Optical imaging

Rats were anesthetized with 1.25 g/kg urethane (i.p.) and were fixed in a stereotactic apparatus (Kopf). Craniotomies (diameter ~ 1mm) were performed above the S1 forepaw representation (according to (Paxinos and Watson, 1986)). Expression of ZsYellow1 was assessed using a high-resolution, fiber-based confocal microscope (Cellvizio, Mauna Kea Technologies). Fluorescent signal was sampled with a 650- $\mu\text{m}$  diameter fiber optic probe (Mauna Kea Technologies), providing a field of view of  $600 \times 500 \mu\text{m}$  with a spatial resolution of 3.3  $\mu\text{m}$ . For simultaneous recording of ZsYellow1 expression and extracellular electrophysiological recordings, a 350-K $\Omega$  tungsten electrode (FHC) was coupled with the optic microprobe and lowered to the cortical layer V of S1 (0 mm AP, 3.8 mm ML, 1 mm DV) using micromanipulators (FHC). Real-time video at the rate of nine frames per second (fps) was captured by ImageCell 3.8 software (Mauna Kea Technologies). To reduce photobleaching, 10 frames were sampled every 30 seconds. Following a baseline recording of 15 minutes, stimulation of the intact forepaw was delivered with 3mA 300- $\mu\text{s}$  pulses repeated at 3Hz for three min. Sensory stimulations were repeated seven times every eight minutes and were coupled with Local field potential (LFP) recordings. LFP was sampled at 1 kHz and bandpass-filtered between 0.1–500 Hz. Discriminated signals were collected with a Cambridge Electronic Design (CED) interface and Spike2 (CED) data acquisition and analysis software.

### Data processing and statistics

Optical imaging recordings were analyzed using Matlab (The MathWorks). Quantitative analysis of ZsYellow1 expression was performed using in-house Matlab scripts by calculating the slope of fluorescence signals (Fischer et al., 2006; Euler et al., 2012; Srinivasan et al., 2012; Srinivasan et al., 2013). Each single recording consisted of 10 frames and these were averaged into one image in order to reduce the size of the dataset. Changes in fluorescence were determined for each pixel by calculating the changes in signal intensity over 15-minute segments (signal intensity (SI) /min, i.e., slope). Pixels that showed increases greater than 0.3 SI/minute in the first segment, where sensory stimulation was presented, and an overall positive increase throughout the stimulation period, were further included in the analysis. Immunohistochemistry analysis (see details below) revealed that the diameter of cells that showed increases in *c-fos* was  $19.0 \pm 4.0 \mu\text{m}$ . Therefore, clusters of pixels that contained more than 13 pixels, for a total diameter of 16.5  $\mu\text{m}$ , were regarded as showing stimulation-induced increases in *c-fos*. The difference in the mean number of clusters between each of the hemispheres in the denervated and the control rats was tested using the Wilcoxon-Mann-Whitney test. LFP waveforms were averaged with respect to the stimulation triggers. The mean amplitude of the evoked LFP response was determined for each series of stimulations. The difference in maximal amplitude between the denervated and the control rats was tested using a Wilcoxon-Mann-Whitney test. All statistical analysis

was overseen by a biostatistician from the Johns Hopkins Bloomberg School of Public Health.

### Immunohistochemistry

Immunostaining of free-floating, 50  $\mu\text{m}$ -thick axial sections was performed using mouse anti-V5 (1:500, Invitrogen), rabbit anti-NeuN (1:1000, Millipore), and rabbit anti-*c-fos* (1:500, Santa Cruz Biotechnology) primary antibodies, and goat anti-rabbit (1:1000; Molecular Probes), goat anti-mouse (1:1000; Molecular Probes) secondary antibodies, and DAPI (Molecular Probes). An Axio Imager.M2 upright equipped with an AxioCam MR3 monochrome CCD camera (Zeiss).was used to image stained slices.

## Results

### *In vitro* measurements of *c-fos* expression

In order to image real-time changes at the transcriptional level after peripheral nerve injury, we engineered a new reporter system. We initially cloned the *c-fos* promoter (position  $-379$  to  $+119$  with respect to the *c-fos* gene (Susini et al., 2000)) from rat genomic DNA. This promoter can be induced via activation of both the cAMP-responsive (CRE) and the serum-responsive (SRE) promoter elements. Next, we constructed a lentivirus encoding to the yellow fluorescent protein (ZsYellow1) fused to the epitope V5 under the regulation of the *c-fos* promoter (pLenti-*c-fos*-ZsYellow-V5).

We measured the kinetics of the ZsYellow1 expression in culture, in SH-SY5Y cells, in response to the phorbol ester, 12-O-tetradecanoylphorbol-13-acetate (TPA), a known activator of the *c-fos* gene (Castagna et al., 1982; Olsson et al., 2000). SH-SY5Y cells transfected with pLenti-6-*c-fos*-ZsYellow1-V5 showed a rapid increase in fluorescence that led to a visible fluorescence in approximately 50% of transfected cells within 15 minutes, and a significantly higher signal within 45 minutes after activation (Figure 1A;  $p$ -value $<0.01$ ). After one hour, the normalized fluorescent signal intensity increased significantly from  $0.23\pm 0.2$  to  $29.40\pm 5.2$  (Figure 1 B and C;  $p$ -value $<0.01$ ). Control cells that were transfected, but treated only with the solvent (DMSO), showed no changes in fluorescence. These findings indicate that the *c-fos* promoter can drive the reporter gene expression on a time scale of 15-45 minutes, and thus, is suitable for reporting real time changes in gene expression *in vivo*.

### *In vivo* measurements of *c-fos* expression

To investigate whether cortical plasticity following peripheral nerve injury results in an elevation of early immediate genes expression, a lentivirus carrying a pLenti-6-*c-fos*-ZsYellow1-V5 construct was delivered into the lateral ventricles of two-day-old rats ( $n=20$ ). At the age of five weeks, 10 rats underwent unilateral limb denervation, and reorganization of the primary somatosensory cortex (S1) was assessed two-to-three weeks later by simultaneous recording of fluorescent optical imaging of ZsYellow1 expression, driven by the *c-fos* promoter, and local field potential (LFP) evoked responses to forepaw sensory stimulation.

To measure gene expression in stimulated cells, which manifested by increased fluorescence, we computed the slope of the fluorescence signal. In this analysis, the rate of fluorescence change is calculated as a function of time. A set number of neighboring pixels that showed simultaneous elevation in fluorescence were clustered together and counted as one responding cell. Figure 2 demonstrates that the clustered pixels had a shape, size, and distribution similar to cells expressing the pLenti-6-*c-fos*-ZsYellow1-V5. The average cluster size was  $12.1 \pm 4 \mu\text{m}$  and contained  $23.0 \pm 14$  pixels, which corresponds to the size of neurons in S1, as was validated by immunohistochemistry analysis of axial brain sections (Figure 2).

We collected continuous optical and electrophysiological data for 66 min, including 15 min of baseline recording and seven three-minute sensory limb stimulations separated by five-minute intervals of rest. Figure 3 shows real-time measurements of ZsYellow1 by fiber-based confocal microscope coupled with a tungsten electrode in layer V of S1.

As anticipated, in control rats, stimulation of the forepaw resulted in increases in the number of fluorescent cells and evoked LFP responses in S1 contralateral to stimulation (Table 1, Figure 3 B and D;  $13.4 \pm 3$  cells and  $0.549 \pm 0.06$  mV, respectively). No optical or electrophysiological responses were observed in S1 ipsilateral to stimulation ( $1.0 \pm 1$  cells and  $0.054 \pm 0.02$  mV, respectively). However, in denervated rats, stimulation of the intact forepaw resulted in significant increases in the number of fluorescent cells in S1, both contralateral ( $27.6 \pm 3$  cells) and ipsilateral ( $8.6 \pm 3$  cells) to stimulation, compared to controls (both  $p\text{-value} < 0.05$ ). Furthermore, in the denervated rats, intact forepaw stimulation resulted in evoked LFP responses in S1 contralateral to stimulation ( $1.315 \pm 0.22$  mV), but no significant changes in S1 ipsilateral to stimulation ( $0.103 \pm 0.03$  mV;  $p\text{-value} > 0.05$ , Figure 3 D and E). These results indicate that post-injury plasticity involves changes at the transcriptional level.

### **Ex vivo validation of *in vivo* results**

Double staining against the V5 tag and the neuronal marker, NeuN, in activated S1 areas showed an overlap between the two markers, indicating that the *c-fos*-ZsYellow1-V5 was expressed in neurons (Figure 4A). Three independent experiments showed that  $50.9 \pm 13.5\%$  of transduced cells were neurons. This is in line with previous reports that demonstrated that both neurons and non-neuronal cell types express *c-fos* (Dragunow and Faull, 1989). Figure 4B demonstrates that *c-fos*-ZsYellow1-V5 and the endogenous *c-fos* largely coincide within the same cells. Cell counting in three brain slices obtained from three different animals showed that  $62.9 \pm 28.3\%$  of the V5 tag positive cells are also positive for endogenous *c-fos*.

### **Discussion**

Nerve injury often results in significant and long-term changes in neuronal activity, which is manifested by altered electrophysiological and functional magnetic resonance imaging (fMRI) responses in cortical areas contralateral and ipsilateral to the injury (Pelled et al., 2007; Pelled et al., 2009; Pawela et al., 2010; Li et al., 2011; Han et al., 2013). While evidence suggests that these neurophysiological changes correlate with the degree of sensory dysfunction and pain in patients (Flor et al., 1995; Lundborg, 2003; Ephraim et al., 2005;

Navarro et al., 2007), the cellular mechanisms leading to these neuronal alterations remain unclear. A variety of transcription factors, neuropeptides, and ion channel expression have been implicated in post-injury plasticity (reviewed by (Navarro et al., 2007)) and the chronic pain associated with these conditions (reviewed by (Kuner, 2010)). Advances in microarray technologies have been shown to be a valuable tool with which to identify differentially expressed genes associated with injury. However, a technique that would allow visualization of proteins associated with plasticity, together with functional assays *in vivo*, could prove to be a powerful tool in elucidating the cellular mechanisms that are activated post-injury and in understanding how these mechanisms are involved in reshaping neuronal networks. Here, we demonstrate a new platform with which to image real-time changes in gene expression, with simultaneous neurophysiological recordings in a living animal.

We utilized fiber-based confocal microscopy technology to detect the fluorescent protein, ZsYellow1, driven by the *c-fos* promoter. The fiber-based confocal microscope has been used previously to monitor *in vivo* regeneration of peripheral nerves (Pelled et al., 2006; Vincent et al., 2006), and to follow the migration of stem cells in the brain (Sumner et al., 2009). This allowed us to overcome the superficial imaging that limits traditional microscopy. Enhanced ZsYellow1 expression was obtained by using an optimized *c-fos* promoter, leading to 16-fold increases in mRNA accumulation via activation of the cAMP-responsive (CRE) and the serum-responsive (SRE) promoter elements (Susini et al., 2000). *C-fos* expression has been shown to significantly increase in the CNS as a response to various physiological stimuli (Tian and Bishop, 2002) (Lin et al., 2011) (Curran and Morgan, 1995; Dampney et al., 1995; Cunningham et al., 2002). Previous studies obtained *in vitro* have shown that *c-fos* mRNA expression can be observed within five minutes following stimulation, and peaks 10-20 minutes after stimulation (Greenberg and Ziff, 1984; Flavell and Greenberg, 2008). Increases in the accumulation of *c-fos* protein *in vivo* in response to limb (Munzlani and Hunt, 1995), limb injury (Gu et al., 1997), vibrissa (Chaudhuri et al., 2000), auditory (Ehret and Fischer, 1991; Clarkson et al., 2010), and visual (Kaczmarek et al., 1999; Chaudhuri et al., 2000) stimulation have been shown to occur as early as 15 minutes after chemical or electrical stimulation in both neurons and glial cells, and peak 60-120 min after stimulation (Tian and Bishop, 2002). In line with the latter findings, our immunohistochemistry results demonstrated that only 60% of infected cells expressed *c-fos*, suggesting that our construct may have been expressed in non-neuronal cells as well (i.e. glia and vascular cells).

An important characteristic of *c-fos* is that, compared to other members of IEG, it expresses in both excitatory and inhibitory neurons (Menetrey et al., 1989; Lanahan and Worley, 1998). Nevertheless, upregulation of *c-fos* activity is often accompanied by an increase in additional IEG-like Zif268 (Egr1) and activity-regulated cytoskeleton-associated protein (Arc) (Tse et al., 2011). However, evidence suggests that the degree of increases in *c-fos* levels serves a good predictor of various plasticity mechanisms. For example, while plasticity-associated expression of Zif268, Arc, and *c-fos* was similar in the hippocampal and the cortical neurons, only Arc and *c-fos* mRNA levels were correlated across structures (Guzowski et al., 2001). Furthermore, *c-fos* mRNA levels were found to be sensitive to adaptation compared to other IEG in a repeated immobilization rat model (Ons et al., 2010).

Other studies have shown that increased expression of Zif268, Arc, and *c-fos* are observed during long-term potentiation, but only *c-fos* expression significantly increases during long-term depression, allowing detection of both enhancement and reduction in the efficacy of synapses (Yilmaz-Rastoder et al., 2011; Ranieri et al., 2012; Kemp et al., 2013). Recently, a neuronal activity-dependent enhancer, the synaptic activity-responsive element (SARE) that regulates the induction of Arc by three activity-dependent transcription factors, was identified (Kawashima et al., 2009). Using a modular engineering approach, an enhanced version of the SARE promoter (E-SARE) was developed, which drives downstream expression at much higher levels compared to previous IEG promoters (Kawashima et al., 2013). Although several other IEG promoters recently became popular markers of neuronal activity, the *c-fos* promoter is commonly used to validate findings. While the majority of imaging-based studies have focused on optical markers to monitor *c-fos* gene regulation, it should be noted that other means, such as magnetic resonance imaging (MRI), have been used to non-invasively monitor *c-fos* (Liu et al., 2007) and fosB mRNA *in vivo* (Liu et al., 2009). It has been suggested that genetically encoded reporters designed for MRI (Gilad et al., 2007; Bar-Shir et al., 2013), and driven by the *c-fos* promoter, can be applied for the real-time monitoring of gene expression in a similar manner. This approach has the potential to provide macroscopic information that can be co-registered with gross anatomical and functional data (Jasanoff, 2007).

In agreement with previous reports, we have shown *in vitro* that the recombinant *c-fos* promoter can successfully drive the inducible expression of ZsYellow1 in SH-SY5Y. Increases in the fluorescent signal were detected starting at 15 minutes after activation. We then sought to determine whether up-regulation of *c-fos* expression could be detected *in vivo*. We specifically probed the cortical layer V of S1 since we previously observed that injury results in long-term up-regulation of the activity of inhibitory interneurons located in that cortical layer. Our results demonstrate that injury leads to a significant stimulation-induced increase in the expression levels of the *c-fos* gene in S1, both contralateral and ipsilateral to the injured limb. In line with our previous observations (Pelled et al., 2009; Li et al., 2011), increases in *c-fos* expression in the affected S1, contralateral to the injured limb, were not accompanied by increases in evoked LFP responses. Since LFP are believed to measure the averaged excitatory synaptic activity in the vicinity of the electrode (Mitzdorf, 1985), it is plausible that the up-regulation of *c-fos* expression in the affected S1 occurs specifically in inhibitory interneurons. Indeed, human studies suggest that an increase in inhibitory neuronal activity in the affected cortex might be the foundation of the poor recovery, sensory dysfunctions, and pain observed in patients who suffer from nerve injury (Karl et al., 2001; Werhahn et al., 2002). Moreover, using optogenetics tools in denervated rats, we observed an immediate increase in excitatory neuronal function and fMRI responses in the infragranular layers of the affected S1 (Li et al., 2011). Nevertheless, future technical development that will allow expression of ZsYellow1, together with specific labeling of neuronal types, will be required to validate this observation.

## Conclusion

Building upon previous findings, which showed that peripheral nerve injury results in cortical plasticity in layer V of S1 contralateral to the injured limb, we showed here that



post-injury plasticity is manifested by an increase in *c-fos* expression, most probably in inhibitory interneurons. Further studies should be directed toward elucidating the effect of post-injury plasticity at the epigenetic level.

## Acknowledgments

The authors declare no competing financial interests. This study was supported by R01NS072171, R01NS079288, and MSCRFII-0042. The authors thank Dr. Alan Koretsky (NIH/NINDS) for providing the Cellvizio and Ms. Mary McAllister for editing the manuscript.

## References

- Bar-Shir A, Liu G, Greenberg MM, Bulte JWM, Gilad AA. Synthesis of a probe for monitoring HSV1-tk reporter gene expression using chemical exchange saturation transfer MRI. *Nat Protocols*. 2013; 8:2380–2391.
- Barth AL, Gerkin RC, Dean KL. Alteration of neuronal firing properties after in vivo experience in a FosGFP transgenic mouse. *J Neurosci*. 2004; 24:6466–6475. [PubMed: 15269256]
- Castagna M, Takai Y, Kaibuchi K, Sano K, Kikkawa U, Nishizuka Y. Direct activation of calcium-activated, phospholipid-dependent protein kinase by tumor-promoting phorbol esters. *J Biol Chem*. 1982; 257:7847–7851. [PubMed: 7085651]
- Chaudhuri A, Zangenehpour S, Rahbar-Dehgan F, Ye F. Molecular maps of neural activity and quiescence. *Acta Neurobiol Exp (Wars)*. 2000; 60:403–410. [PubMed: 11016083]
- Cifani C, Koya E, Navarre BM, Calu DJ, Baumann MH, Marchant NJ, Liu QR, Khuc T, Pickel J, Lupica CR, Shaham Y, Hope BT. Medial prefrontal cortex neuronal activation and synaptic alterations after stress-induced reinstatement of palatable food seeking: a study using c-fos-GFP transgenic female rats. *J Neurosci*. 2012; 32:8480–8490. [PubMed: 22723688]
- Clarkson C, Juiz JM, Merchan MA. Transient Down-Regulation of Sound-Induced c-Fos Protein Expression in the Inferior Colliculus after Ablation of the Auditory Cortex. *Front Neuroanat*. 2010; 4:141. [PubMed: 21088696]
- Cunningham JT, Grindstaff RJ, Grindstaff RR, Sullivan MJ. Fos immunoreactivity in the diagonal band and the perinuclear zone of the supraoptic nucleus after hypertension and hypervolaemia in unanaesthetized rats. *J Neuroendocrinol*. 2002; 14:219–227. [PubMed: 11999722]
- Curran T, Morgan JI. Fos: an immediate-early transcription factor in neurons. *J Neurobiol*. 1995; 26:403–412. [PubMed: 7775973]
- Dampney RA, Li YW, Hirooka Y, Potts P, Polson JW. Use of c-fos functional mapping to identify the central baroreceptor reflex pathway: advantages and limitations. *Clin Exp Hypertens*. 1995; 17:197–208. [PubMed: 7735269]
- Dragunow M, Faull R. The use of c-fos as a metabolic marker in neuronal pathway tracing. *J Neurosci Methods*. 1989; 29:261–265. [PubMed: 2507830]
- Ehret G, Fischer R. Neuronal activity and tonotopy in the auditory system visualized by c-fos gene expression. *Brain Res*. 1991; 567:350–354. [PubMed: 1817741]
- Ephraim PL, Wegener ST, MacKenzie EJ, Dillingham TR, Pezzin LE. Phantom pain, residual limb pain, and back pain in amputees: results of a national survey. *Arch Phys Med Rehabil*. 2005; 86:1910–1919. [PubMed: 16213230]
- Euler M, Wang Y, Otto P, Tomaso H, Escudero R, Anda P, Hufert FT, Weidmann M. Recombinase polymerase amplification assay for rapid detection of *Francisella tularensis*. *J Clin Microbiol*. 2012; 50:2234–2238. [PubMed: 22518861]
- Fischer T, Gemeinhardt I, Wagner S, Stieglitz DV, Schnorr J, Hermann KG, Ebert B, Petzelt D, Macdonald R, Licha K, Schirner M, Krenn V, Kamradt T, Taupitz M. Assessment of unspecific near-infrared dyes in laser-induced fluorescence imaging of experimental arthritis. *Acad Radiol*. 2006; 13:4–13. [PubMed: 16399028]
- Flavell SW, Greenberg ME. Signaling mechanisms linking neuronal activity to gene expression and plasticity of the nervous system. *Annu Rev Neurosci*. 2008; 31:563–590. [PubMed: 18558867]

- Fleischmann A, Hvalby O, Jensen V, Strekalova T, Zacher C, Layer LE, Kvello A, Reschke M, Spanagel R, Sprengel R, Wagner EF, Gass P. Impaired long-term memory and NR2A-type NMDA receptor-dependent synaptic plasticity in mice lacking c-Fos in the CNS. *J Neurosci*. 2003; 23:9116–9122. [PubMed: 14534245]
- Flor H, Elbert T, Knecht S, Wienbruch C, Pantev C, Birbaumer N, Larbig W, Taub E. Phantom-limb pain as a perceptual correlate of cortical reorganization following arm amputation. *Nature*. 1995; 375:482–484. [PubMed: 7777055]
- Fujihara H, Ueta Y, Suzuki H, Katoh A, Ohbuchi T, Otsubo H, Dayanithi G, Murphy D. Robust up-regulation of nuclear red fluorescent-tagged fos marks neuronal activation in green fluorescent vasopressin neurons after osmotic stimulation in a double-transgenic rat. *Endocrinology*. 2009; 150:5633–5638. [PubMed: 19850746]
- Gilad AA, McMahon MT, Walczak P, Winnard PT Jr, Raman V, van Laarhoven HW, Skoglund CM, Bulte JW, van Zijl PC. Artificial reporter gene providing MRI contrast based on proton exchange. *Nat Biotechnol*. 2007; 25:217–219. [PubMed: 17259977]
- Greenberg ME, Ziff EB. Stimulation of 3T3 cells induces transcription of the c-fos proto-oncogene. *Nature*. 1984; 311:433–438. [PubMed: 6090941]
- Gu ZZ, Pan YC, Cui JK, Klebuc MJ, Shenaq S, Liu PK. Gene expression and apoptosis in the spinal cord neurons after sciatic nerve injury. *Neurochem Int*. 1997; 30:417–426. [PubMed: 9106256]
- Guzowski JF, Setlow B, Wagner EK, McGaugh JL. Experience-dependent gene expression in the rat hippocampus after spatial learning: a comparison of the immediate-early genes Arc, c-fos, and zif268. *J Neurosci*. 2001; 21:5089–5098. [PubMed: 11438584]
- Han Y, Li N, Zeiler SR, Pelled G. Peripheral nerve injury induces immediate increases in layer v neuronal activity. *Neurorehabil Neural Repair*. 2013; 27:664–672. [PubMed: 23599222]
- Jasanoff A. MRI contrast agents for functional molecular imaging of brain activity. *Curr Opin Neurobiol*. 2007; 17:593–600. [PubMed: 18093824]
- Kaczmarek L, Zangenehpour S, Chaudhuri A. Sensory regulation of immediate-early genes c-fos and zif268 in monkey visual cortex at birth and throughout the critical period. *Cereb Cortex*. 1999; 9:179–187. [PubMed: 10220230]
- Karl A, Birbaumer N, Lutzenberger W, Cohen LG, Flor H. Reorganization of motor and somatosensory cortex in upper extremity amputees with phantom limb pain. *J Neurosci*. 2001; 21:3609–3618. [PubMed: 11331390]
- Kasof GM, Mandelzys A, Maika SD, Hammer RE, Curran T, Morgan JJ. Kainic acid-induced neuronal death is associated with DNA damage and a unique immediate-early gene response in c-fos-lacZ transgenic rats. *J Neurosci*. 1995; 15:4238–4249. [PubMed: 7790908]
- Kawashima T, Okuno H, Nonaka M, Adachi-Morishima A, Kyo N, Okamura M, Takemoto-Kimura S, Worley PF, Bito H. Synaptic activity-responsive element in the Arc/Arg3.1 promoter essential for synapse-to-nucleus signaling in activated neurons. *Proc Natl Acad Sci U S A*. 2009; 106:316–321. [PubMed: 19116276]
- Kawashima T, Kitamura K, Suzuki K, Nonaka M, Kamijo S, Takemoto-Kimura S, Kano M, Okuno H, Ohki K, Bito H. Functional labeling of neurons and their projections using the synthetic activity-dependent promoter E-SARE. *Nat Methods*. 2013; 10:889–895. [PubMed: 23852453]
- Kemp A, Tischmeyer W, Manahan-Vaughan D. Learning-facilitated long-term depression requires activation of the immediate early gene, c-fos, and is transcription dependent. *Behav Brain Res*. 2013; 254:83–91. [PubMed: 23644186]
- Kuner R. Central mechanisms of pathological pain. *Nat Med*. 2010; 16:1258–1266. [PubMed: 20948531]
- Lanahan A, Worley P. Immediate-early genes and synaptic function. *Neurobiol Learn Mem*. 1998; 70:37–43. [PubMed: 9753585]
- Li N, Downey JE, Bar-Shir A, Gilad AA, Walczak P, Kim H, Joel SE, Pekar JJ, Thakor NV, Pelled G. Optogenetic-guided cortical plasticity after nerve injury. *Proc Natl Acad Sci U S A*. 2011; 108:8838–8843. [PubMed: 21555573]
- Lin HY, Tang CH, Chen JH, Chuang JY, Huang SM, Tan TW, Lai CH, Lu DY. Peptidoglycan induces interleukin-6 expression through the TLR2 receptor, JNK, c-Jun, and AP-1 pathways in microglia. *J Cell Physiol*. 2011; 226:1573–1582. [PubMed: 20945380]

- Liu CH, Kim YR, Ren JQ, Eichler F, Rosen BR, Liu PK. Imaging cerebral gene transcripts in live animals. *J Neurosci*. 2007; 27:713–722. [PubMed: 17234603]
- Liu CH, Ren JQ, Yang J, Liu CM, Mandeville JB, Rosen BR, Bhide PG, Yanagawa Y, Liu PK. DNA-based MRI probes for specific detection of chronic exposure to amphetamine in living brains. *J Neurosci*. 2009; 29:10663–10670. [PubMed: 19710318]
- Liu X, Ramirez S, Pang PT, Puryear CB, Govindarajan A, Deisseroth K, Tonegawa S. Optogenetic stimulation of a hippocampal engram activates fear memory recall. *Nature*. 2012; 484:381–385. [PubMed: 22441246]
- Lundborg G, Richard P. Bunge memorial lecture. Nerve injury and repair--a challenge to the plastic brain. *J Peripher Nerv Syst*. 2003; 8:209–226. [PubMed: 14641646]
- Menetrey D, Gannon A, Levine JD, Basbaum AI. Expression of c-fos protein in interneurons and projection neurons of the rat spinal cord in response to noxious somatic, articular, and visceral stimulation. *J Comp Neurol*. 1989; 285:177–195. [PubMed: 2503547]
- Milde-Langosch K. The Fos family of transcription factors and their role in tumourigenesis. *Eur J Cancer*. 2005; 41:2449–2461. [PubMed: 16199154]
- Mitzdorf U. Current source-density method and application in cat cerebral cortex: investigation of evoked potentials and EEG phenomena. *Physiol Rev*. 1985; 65:37–100. [PubMed: 3880898]
- Munglani R, Hunt SP. Molecular biology of pain. *Br J Anaesth*. 1995; 75:186–192. [PubMed: 7577252]
- Navarro X, Vivo M, Valero-Cabre A. Neural plasticity after peripheral nerve injury and regeneration. *Prog Neurobiol*. 2007; 82:163–201. [PubMed: 17643733]
- Olsson AK, Vadhammar K, Nanberg E. Activation and protein kinase C-dependent nuclear accumulation of ERK in differentiating human neuroblastoma cells. *Exp Cell Res*. 2000; 256:454–467. [PubMed: 10772818]
- Ons S, Rotllant D, Marin-Blasco IJ, Armario A. Immediate-early gene response to repeated immobilization: Fos protein and arc mRNA levels appear to be less sensitive than c-fos mRNA to adaptation. *Eur J Neurosci*. 2010; 31:2043–2052. [PubMed: 20608965]
- Pawela CP, Biswal BB, Hudetz AG, Li R, Jones SR, Cho YR, Matloub HS, Hyde JS. Interhemispheric neuroplasticity following limb deafferentation detected by resting-state functional connectivity magnetic resonance imaging (fcMRI) and functional magnetic resonance imaging (fMRI). *Neuroimage*. 2010; 49:2467–2478. [PubMed: 19796693]
- Paxinos, G.; Watson, C. *The rat brain in stereotaxic coordinates*. 2nd Edition. Academic Press; Sydney; Orlando: 1986.
- Pelled G, Dodd SJ, Koretsky AP. Catheter confocal fluorescence imaging and functional magnetic resonance imaging of local and systems level recovery in the regenerating rodent sciatic nerve. *Neuroimage*. 2006; 30:847–856. [PubMed: 16343952]
- Pelled G, Chuang KH, Dodd SJ, Koretsky AP. Functional MRI detection of bilateral cortical reorganization in the rodent brain following peripheral nerve deafferentation. *Neuroimage*. 2007; 37:262–273. [PubMed: 17544301]
- Pelled G, Bergstrom DA, Tierney PL, Conroy RS, Chuang KH, Yu D, Leopold DA, Walters JR, Koretsky AP. Ipsilateral cortical fMRI responses after peripheral nerve damage in rats reflect increased interneuron activity. *Proc Natl Acad Sci U S A*. 2009; 106:14114–14119. [PubMed: 19666522]
- Ranieri F, Podda MV, Riccardi E, Frisullo G, Dileone M, Profice P, Pilato F, Di Lazzaro V, Grassi C. Modulation of LTP at rat hippocampal CA3-CA1 synapses by direct current stimulation. *J Neurophysiol*. 2012; 107:1868–1880. [PubMed: 22236710]
- Reijmers LG, Perkins BL, Matsuo N, Mayford M. Localization of a stable neural correlate of associative memory. *Science*. 2007; 317:1230–1233. [PubMed: 17761885]
- Srinivasan VJ, Radhakrishnan H, Jiang JY, Barry S, Cable AE. Optical coherence microscopy for deep tissue imaging of the cerebral cortex with intrinsic contrast. *Opt Express*. 2012; 20:2220–2239. [PubMed: 22330462]
- Srinivasan VJ, Mandeville ET, Can A, Blasi F, Klimov M, Daneshmand A, Lee JH, Yu E, Radhakrishnan H, Lo EH, Sakadzic S, Eikermann-Haerter K, Ayata C. Multiparametric,

- longitudinal optical coherence tomography imaging reveals acute injury and chronic recovery in experimental ischemic stroke. *PLoS One*. 2013; 8:e71478. [PubMed: 23940761]
- Sumner JP, Shapiro EM, Maric D, Conroy R, Koretsky AP. In vivo labeling of adult neural progenitors for MRI with micron sized particles of iron oxide: quantification of labeled cell phenotype. *Neuroimage*. 2009; 44:671–678. [PubMed: 18722534]
- Susini S, Van Haasteren G, Li S, Prentki M, Schlegel W. Essentiality of intron control in the induction of c-fos by glucose and glucoincretin peptides in INS-1 beta-cells. *FASEB J*. 2000; 14:128–136. [PubMed: 10627287]
- Tian JB, Bishop GA. Stimulus-dependent activation of c-Fos in neurons and glia in the rat cerebellum. *J Chem Neuroanat*. 2002; 23:157–170. [PubMed: 11861123]
- Tse D, Takeuchi T, Kakeyama M, Kajii Y, Okuno H, Tohyama C, Bito H, Morris RG. Schema-dependent gene activation and memory encoding in neocortex. *Science*. 2011; 333:891–895. [PubMed: 21737703]
- Vincent P, Maskos U, Charvet I, Bourgeais L, Stoppini L, Leresche N, Changeux JP, Lambert R, Meda P, Paupardin-Tritsch D. Live imaging of neural structure and function by fibred fluorescence microscopy. *EMBO Rep*. 2006; 7:1154–1161. [PubMed: 17008931]
- Wada M, Watanabe S, Chung UI, Higo N, Taniguchi T, Kitazawa S. Noninvasive bioluminescence imaging of c-fos expression in the mouse barrel cortex. *Behav Brain Res*. 2010; 208:158–162. [PubMed: 19931567]
- Werhahn KJ, Mortensen J, Kaelin-Lang A, Boroojerdi B, Cohen LG. Cortical excitability changes induced by deafferentation of the contralateral hemisphere. *Brain*. 2002; 125:1402–1413. [PubMed: 12023328]
- Wilson Y, Nag N, Davern P, Oldfield BJ, McKinley MJ, Greferath U, Murphy M. Visualization of functionally activated circuitry in the brain. *Proc Natl Acad Sci U S A*. 2002; 99:3252–3257. [PubMed: 11867719]
- Yasoshima Y, Morimoto T, Yamamoto T. Different disruptive effects on the acquisition and expression of conditioned taste aversion by blockades of amygdalar ionotropic and metabotropic glutamatergic receptor subtypes in rats. *Brain Res*. 2000; 869:15–24. [PubMed: 10865054]
- Yilmaz-Rastoder E, Miyamae T, Braun AE, Thiels E. LTP- and LTD-inducing stimulations cause opposite changes in arc/arg3.1 mRNA level in hippocampal area CA1 in vivo. *Hippocampus*. 2011; 21:1290–1301. [PubMed: 20824728]

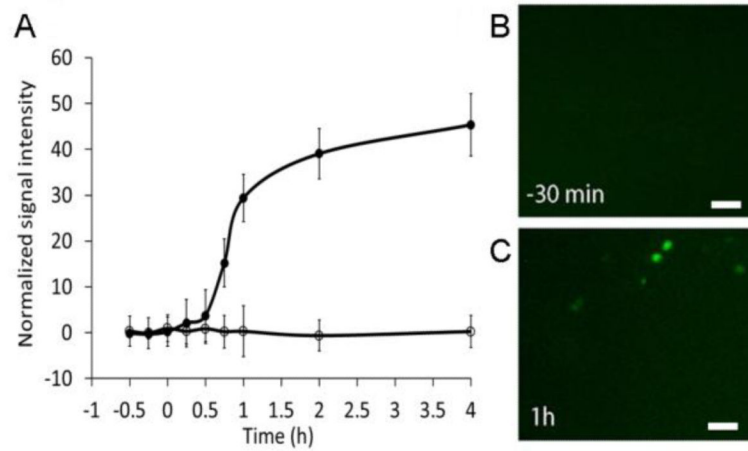


**Figure 1. Induction of *c-fos-ZsYellow1* in vitro**

**A.** Quantification of fluorescence from SH-SY5Y cells transiently transfected with pLenti-6-*c-fos-ZsYellow1-V5*, and treated with TPA (closed circles) or control DMSO (empty circles). Average with SEM represents the number of fluorescent cells counted from three independent experiments. **B.** SH-SY5Y cells 30 minutes before and **(C)** one hour after activation with TPA. Scale bars correspond to 20  $\mu\text{m}$ .

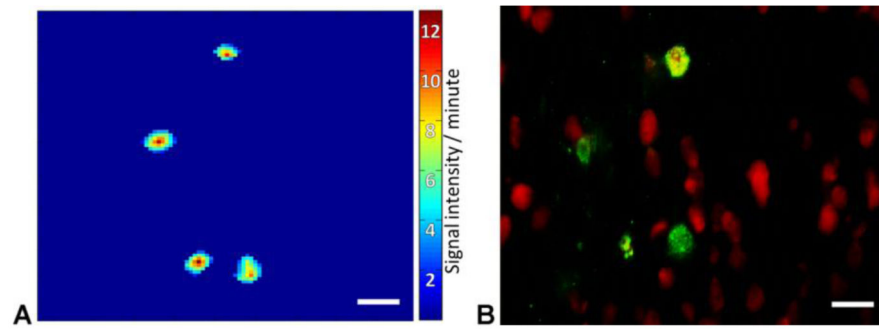


**Figure 2. Fluorescence signal analysis**

**A.** Pixel-by-pixel analysis of signal intensity slopes revealed clusters with a stimulation-specific increase in fluorescence. **B.** Immunohistochemical staining suggests that the size, shape, and distribution of obtained clusters are similar to those of cells expressing pLenti-6-*c-fos*-ZsYellow1-V5 (Anti-V5 in green, NeuN in red). Scale bars correspond to 20  $\mu\text{m}$ .

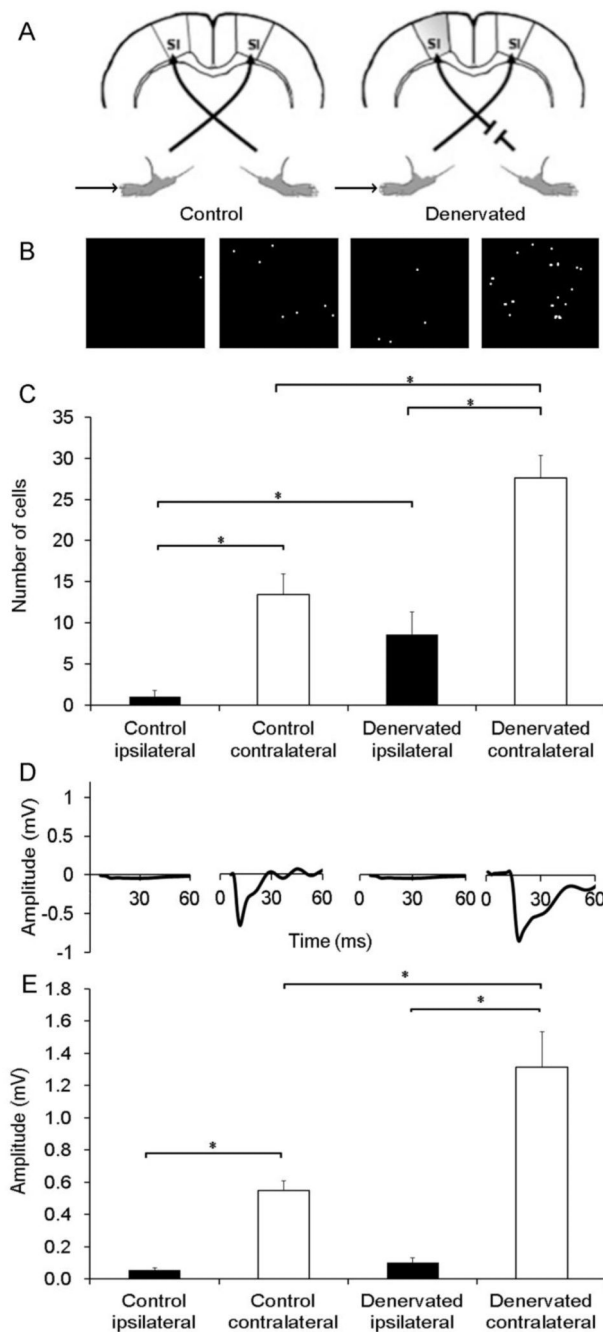


**Figure 3. Real-time increases in *c-fos* expression associated with post-injury plasticity in layer V of S1**

**A.** Schematic experimental paradigm describes the experimental conditions. **B.** Representative optical images of cells, and **(C)** quantification of the number of cells shows increases in fluorescence in S1, both contralateral (white bars) and ipsilateral (black bars) to intact forepaw stimulation in denervated rats compared to controls. Representative evoked LFP **(D)** and quantification of the evoked LFP negative deflection **(E)** demonstrate that forepaw stimulation induced evoked LFP responses in S1 contralateral to stimulation. \* represent a p-value<0.05.

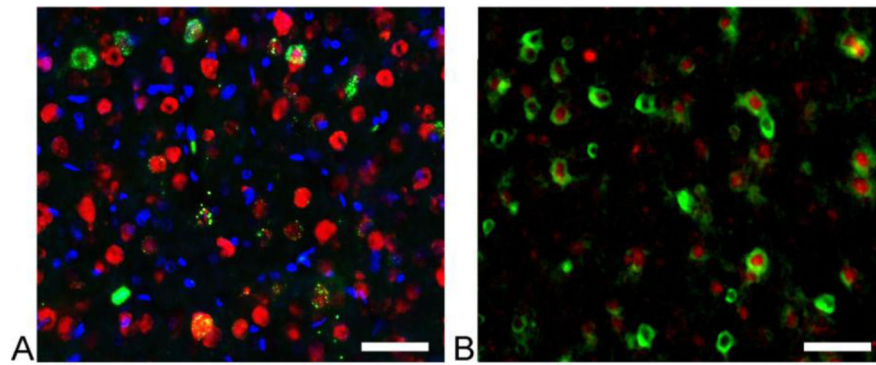


**Figure 4. Immunohistochemical validation of *c-fos-ZsYellow1* expression**

**A.** Expression of *c-fos-ZsYellow1* was verified in S1, contralateral to limb stimulation (anti-V5 – green, NeuN – red, DAPI -blue). **B.** High magnification within S1 suggests co-localization of *c-fos-ZsYellow1* expression with endogenous *c-fos* (anti-V5 - green, *c-fos* - red). Scale bars correspond to 50  $\mu\text{m}$ .



**Table 1**  
**Number of cells showing increases in *c-fos* expression and mean amplitude of evoked LFP responses in denervated and control rats**

The Wilcoxon-Mann-Whitney test was used to compare the responses in S1, contralateral and ipsilateral to stimulation in denervated rats compared to control rats

Control				Denervated			
S1 ipsilateral to stimulation		S1 contralateral to stimulation		S1 ipsilateral to stimulation		S1 contralateral to stimulation	
Number of cells	LFP (mV)	Number of cells	LFP (mV)	Number of cells	LFP (mV)	Number of cells	LFP (mV)
1.0±1*	0.054±0.02	13.4±3*	0.549±0.06*	8.6±3	0.103±0.03	27.6±3	1.315±0.22

\* p-value<0.05.